REFERENCES

[1] D.-C. Chang, C.-B. Chang, and J.-C. Liu, "Modified planar Quasi-Yagi antenna for WLAN dual-band operations," *Microw. Optical Tech. Lett.*, vol. 46, no. 5, pp. 443–446, 2005.

[2] P.-Y. Qin, A. R. Weily, Y. J. Guo, T. S. Bird, and C.-H. Liang, "Frequency reconfigurable Quasi-Yagi folded dipole antenna," *IEEE Trans. Antennas Propag.*, vol. 58, no. 8, pp. 2742–2747, 2010.

[3] J. M. Steyn, J. W. Odendaal, and J. Joubert, "Double dipole antenna for dual-band wireless local area networks applications," *Microw. Optical Tech. Lett.*, vol. 51, no. 9, pp. 2034–2038, 2009.

[4] J. Huang and A. C. Densmore, "Microstrip Yagi array antenna for mobile satellite vehicle application," *IEEE Trans. Antennas Propag.*, vol. 39, no. 7, pp. 1024–1030, 1991.

[5] W. R. Deal, N. Kaneda, J. Sor, Y. Qian, and T. Itoh, "A new Quasi-Yagi antenna for planar active antenna arrays," *IEEE Trans. Microw. Theory Tech.*, vol. 48, no. 6, pp. 910–918, 2000.

[6] N. Kaneda, W. R. Deal, J. Sor, Y. Qian, and T. Itoh, "A broadband planar Quasi-Yagi antenna," *IEEE Trans. Antennas Propag.*, vol. 50, no. 8, pp. 1158–1160, 2002.

[7] T.-G. Ma, C.-W. Wang, R.-C. Hua, and J.-W. Tsai, "A modified Quasi-Yagi antenna with a new compact microstrip-to-coplanar strip transition using artificial transmission lines," *IEEE Trans. Antennas Propag.*, vol. 57, no. 8, pp. 2469–2474, 2009.

[8] F. Landstorfer, "A new type of directional antenna," in *Proc. IEEE Antennas Propag. Soc. Symp.*, Oct. 1976, pp. 169–172.

[9] A. C. K. Mak, C. R. Rowell, and R. D. Murch, "Low cost reconfigurable Landstorfer planar antenna array," *IEEE Trans. Antennas Propag.*, vol. 57, no. 10, pp. 3051–3061, 2009.

[10] *Applications Computer Aided Design Program-AppCAD 2010,* , Agilent Technologies, Inc..

[11] N. Kaneda, Y. Qian, and T. Itoh, "A broadband microstrip-to waveguide transition using Quasi-Yagi antenna," *IEEE Trans. Microw. Theory and Tech.*, vol. 47, no. 12, pp. 2562–2567, 1999.

[12] C. A. Balanis, *Antenna Theory: Analysis and Design*, 2nd ed. Hoboken, NJ: Wiley, 2005, ch. 10.

[13] W. Nannan, Q. Jinghui, L. Shu, and D. Weibo, "Research on wide beamwidth and high gain Quasi-Yagi antenna," in *Proc. 8th Int. Symp. Antennas, Propag. and EM Theory*, Kunming, China, Nov. 2008, pp. 302–305.

[14] *Advanced Design System—ADS 2009* Agilent Technologies.

[15] *High Frequency Structure Simulator—HFSS 2009* Version 11.2, Ansoft, LLC.

[16] W. L. Stutzman and G. A. Thiele, *Antenna Theory and Design*, 2nd ed. New York: Wiley, 1998.

Optimization of UHF Hilbert Antenna for Partial Discharge Detection of Transformers

Jian Li, Tianyan Jiang, Caisheng Wang, and Changkui Cheng

***Abstract*—Partial discharge (PD) online monitoring is an effective tool of inspecting insulation defects and identifying potential faults in power transformers. Ultra-high-frequency (UHF) approaches have caught increasing attention recently and been considered as a promising technology for online monitoring PD signals. The size of a UHF sensor for PD online monitoring of transformer is a critical factor for practical installation inside transformer. This communication presents a compact fourth order UHF Hilbert fractal antenna with desired performance and suitable size for easy installation. Actual PD experiments were carried out for four typical artificial insulation defect models while the antenna was used for PD measurements. The experimental results show that the proposed Hilbert fractal antenna is suitable and effective for UHF online monitoring of PDs in transformers.**

***Index Terms*—Hilbert fractal antenna, partial discharge, transformer, ultra-high-frequency detection.**

I. INTRODUCTION

Power transformers are very important equipment in power systems. A large portion of power transformers failures are caused by faults of oil-paper insulation, which often start with partial discharges (PDs). PDs generate electromagnetic emissions which can be detected by ultra-high-frequency (UHF) antennas in the frequency band greater than 300 MHz [1]. Radio frequency interferences (RFIs) from power line communication and corona discharges on high voltage terminals near transformers can propagate into transformers through high voltage bushings of the transformers and reduce accuracy of PD online monitoring based on principles of traditional PD detection, of which frequency bands are between several tens kHz and several MHz [2]. The frequency bands of RFIs are between a few hundreds kHz and a few tens MHz and the upper frequency limits of the corona discharges do not exceed 300 MHz. The UHF PD detection thus takes advantages of strong anti-interference ability over traditional detection approaches.

The performance of UHF antenna determines the ability of PD online detection systems of high voltage equipment. Currently, various UHF antennas have been used for PD detection. Publication [3] introduced a two-wire Archimedean planar spiral antenna and its application in PD detection. An inverted cone antenna was presented in [4] to measure PD signals in transformer oils. A circular plate antennas and a circular ring antenna were used for PD detection of sulfur hexafluoride

Manuscript received October 13, 2010; revised September 18, 2011; accepted October 26, 2011. Date of publication March 06, 2012; date of current version May 01, 2012. This work was supported in part by the 863 Program (No. 2009AA04Z416) of China, by The National Natural Science Foundation of China (No. 51021005), by the Natural Science Foundation Project of CQ-CSTC, China (CSTC2009BA4048), and in part by the visiting scholar fund supported by SKLPES, Chongqing University, China. The work of C. Wang was supported in part by the National Science Foundation under Award ECS-0823865

J. Li, T. Jiang, and C. Cheng are with the State Key Laboratory of Power Transmission Equipment & System and New Technology, Chongqing University, Chongqing 400044, China (e-mail: lijian@cqu.edu.cn; jiangtianyan@cqu.edu.cn; chengchen3@163.com).

C. Wang is with the Division of Engineering Technology and the Department of Electrical and Computer Engineering, Wayne State University Detroit, MI 48202 USA (e-mail: cwang@wayne.edu).

Color versions of one or more of the figures in this communication are available online at http://ieeexplore.ieee.org.

Digital Object Identifier 10.1109/TAP.2012.2189929

(SF_6) gas insulated high voltage equipment [5]. However, the diameters or side lengths of these UHF antennas are more than 20 cm. They are too difficult to be installed in practical transformers. A third order Hilbert fractal antenna with side length of 30 mm showed good performance for online UHF monitoring of PDs in transformers [6]. But the lowest resonant frequency of the third order Hilbert antenna is 731 MHz [6]. Publications [7] and [8] presented that the number of resonant frequencies of a Hilbert fractal antenna increases and the lowest resonant frequency decreases with increasing of the order of the Hilbert antenna. This motivates us to investigate an optimal design of compact fourth order UHF Hilbert antenna with the lowest resonant frequency approaching 300 MHz for UHF online monitoring of PDs.

This communication presents a fourth order UHF Hilbert fractal antenna for online monitoring of PDs in transformers. This new antenna has a small size and a comparatively wide frequency bandwidth. The design criteria and optimization procedure of the antenna are addressed. The voltage standing wave ratio (VSWR) and radiation patterns of the antenna were obtained through simulation. The performance of the antenna for PD detection was tested through actual PD experiments with four typical artificial insulation defect models in laboratory. The communication is organized as follows: Section II presents the design criteria and the optimization procedures of the UHF PD antenna for power transformers. Section III presents the PD experiments and the experimental results. The conclusion is given in Section IV.

II. Optimal Design of Hilbert Fractal Antenna

A. Design Criteria of PD Antennas

Two criteria have to be considered for design of UHF PD antennas. On one hand, the lowest resonant frequency of a UHF antenna should approach 300 MHz and the frequency bandwidth of the antenna should exceed several hundreds MHz so that PD monitoring sensitivity is high enough and meanwhile the measured signals of PDs can be separated from RFIs and corona discharges. On the other hand, the size of antenna should be small enough not to influence safety of transformers and to be installed in transformers easily in field application. Valves and dielectric windows on transformer tanks are two possible locations for installation of the UHF antenna. The internal diameters of most valves on transformer tanks are smaller than 20 cm. The dielectric windows have to be specially designed and made before delivery of transformers from manufactures to costumers. Their sizes should be as small as possible so that they can be made easily and have no influences to safety of transformers in operation.

It is difficult for a regular communication antenna to satisfy both aspects of the design criteria at the same time. If the frequency bandwidth of a regular communication antenna becomes wider, the size of the antenna has to be increased. However, the Hilbert fractal antenna shows good performance to meet the two criteria [9]. The design of Hilbert fractal antenna is based on Hilbert fractal curve, which is a continuous curve with a characteristic of strict self-similarity. The length of the Hilbert fractal curve increases with increasing of the order of the curve. The Hilbert fractal antenna needs optimization for good performance, which is helpful to be better applied for online monitoring of PD signals in transformers.

B. Optimization of a Fourth Order Hilbert Fractal Antenna

The basic principles of Hilbert fractal antenna was presented in [10]. And the previous research results [11] showed that the performance of a Hilbert fractal antenna was influenced by many factors such as the side dimension L, width of conductor k, thickness b of the printed circuit board (PCB) on which the antenna lies, feed-point, and dielectric constant of the PCB, etc. To obtain an antenna with desired performance,

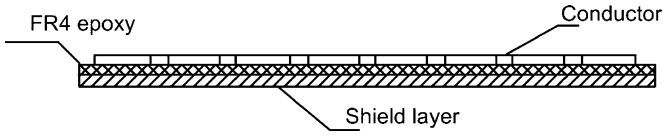

Fig. 1. Simulation model of the Hilbert fractal antenna.

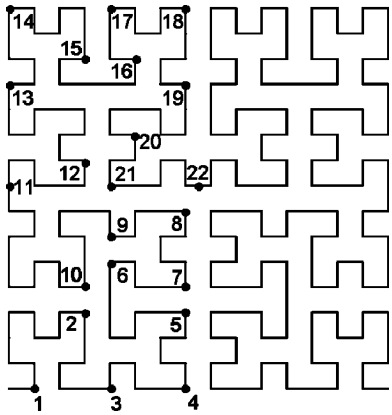

Fig. 2. Feed points selected of Hilbert fractal antenna for simulation.

TABLE I
Values of Parameters of Antenna Selected for Simulation

L (mm)	k (mm)			b (mm)		
	min	Step	max	min	step	max
50	1.0	0.5	2.0	1.0	0.5	4.0
60	1.0	0.5	3.0	1.0	0.5	4.0
75	1.0	0.5	3.0	1.0	0.5	4.0
90	1.0	0.5	3.5	1.0	0.5	4.0
100	1.0	0.5	4.0	1.0	0.5	4.0

the above factors need to be included and optimized in the design procedure. The antenna simulation model in Ansoft is shown in Fig. 1. The antenna contains 3 layers. The top layer is the copper conductor. The middle layer is an insulation board, which is FR4 epoxy board with dielectric constant of 4.4 for simulations as follows. The bottom layer is a copper shield.

The design procedure is depicted as follows. First, five different side dimensions ($L = 50$ mm, 60 mm, 75 mm, 90 mm, 100 mm) of Hilbert antenna were selected for study. For each side dimension L, different widths of conductor given in Table I were explored while other factors are fixed. Other factors such as thickness of PCB, as shown in Table I, and feed points were also analyzed for the gain, radiation pattern and the other performance of the antenna. Since a Hilbert curve is symmetrical, a total of 21 feed points on the left half part of the Hilbert fractal antenna, as shown in Fig. 2, were selected for simulation. Parameter r is defined as the ratio of the distance along the conductor between a feed point and its closest end to the total conduct length of the antenna. For example, the feed point 4 was selected for simulation, and its closest end is the left end of the conductor in Fig. 2. Through the simulations, the parameters of the optimal antenna are determined as $L = 100$ mm, $k = 2$ mm, $b = 1.5$ mm, and $r = 0.082$ corresponding to the feed point 4.

The voltage standing wave ratio (VSWR) and radiation patterns of the antenna are shown in Figs. 3 and 4. Fig. 3 shows that between 0.3 GHz and 1 GHz the multi-band antenna has four frequency bands where $\mathrm{VSWR} < 5$. The bandwidth of the optimal antenna is a few hundred MHz. The two-dimensional radiation patterns at the frequencies of 0.4 GHz, 0.7 GHz, and 1 GHz, are shown in Fig. 4. Its patterns at

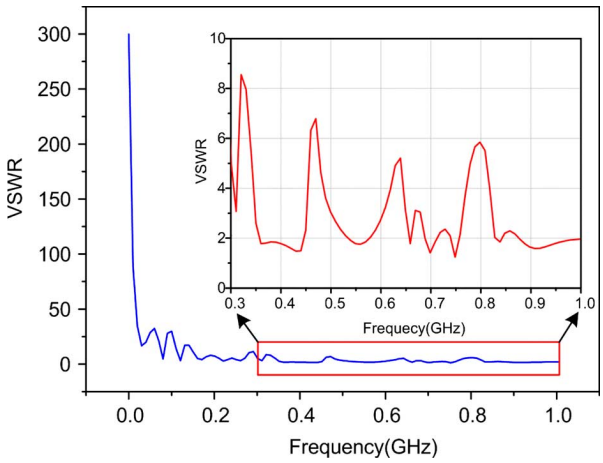

Fig. 3. VWSR curve of the Hilbert fractal antenna.

the three frequencies are all nearly a hemisphere and the gain variations at the three frequencies are relatively stable. Moreover, the simulation results show that the antenna can match with a 50 ohms coaxial cable well in the pass bands. The simulated results show that the optimal Hilbert fractal antenna has small size and wide frequency bandwidth. And the antenna meets the two criteria proposed in Section II.A.

Fig. 4 shows that the minimum gain of the antenna is about -28 dBi. The low gain of the antenna is due to the small size that receiving low energy of the electromagnetic wave. An amplifier and a filter, as shown in Fig. 5, were developed for the wide-band detection in the frequency range between 300 MHz and 1 GHz. The gain of the amplifier is about 40 dB and the gain of the whole system is about 10 dBi.

III. Experiments and Results

The designed Hilbert fractal UHF antenna was used in laboratory for measuring PDs caused by four typical artificial insulation defect models, as shown in Fig. 6. Fig. 6(a) shows the corona discharge model with a needle-to-plate electrode system. Fig. 6(b) shows an experiment model of a cylinder-to-board electrode for surface discharge defects in oil. Fig. 6(c) is the model of air cavity discharge. It consists of three layers of oil-impregnated pressboards and a ball-to-board electrode system. Fig. 6(d) is the model of floating discharge. For this cylinder-to-board electrode system, a metal particle is placed on the paper to simulate a floating electrode. The thickness of the pressboard of each model is 0.5 mm.

Fig. 7 shows the experimental setup of the UHF PD detection. The artificial defect models were placed into an organic glass container filled with transformer oil. The UHF antenna was located in the vicinity of the testing models, with a distance of 50 mm between them. A digital oscilloscope with sampling frequency of 5 GHz was utilized to record the PD signals. The trigger time of the oscilloscope was set to 100 ns. All experiments were carried out in an electromagnetic shielded laboratory.

Table II shows the PD experimental conditions of the four defect models. When the test voltages are lower than the inception voltages, the waves displayed in the oscilloscope are background noise signals, whose amplitudes are about 30 mV. Once the test voltages are higher than the inception voltages, the transient UHF PD signals are captured by the antenna. The number of the PD samples is 50 for each model. One UHF PD signal is obtained at each voltage for every sample.

Because the transient UHF PD signals occur randomly, the frequency spectra among the same defect models vary from each other. However, the differences in frequency spectra that generate from the same defected model are significantly smaller than those in frequency

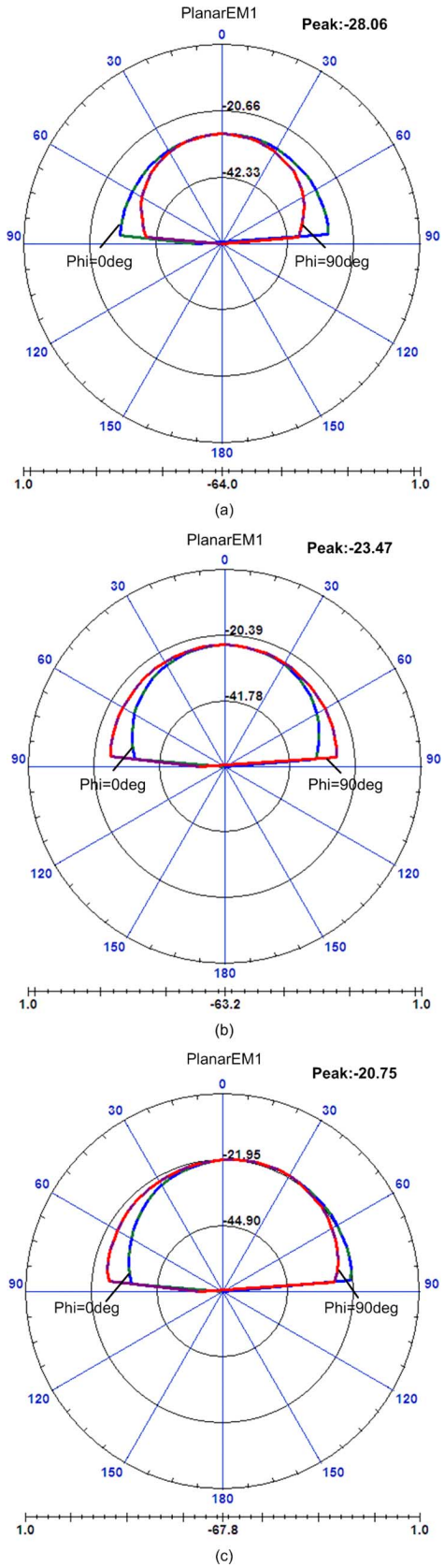

Fig. 4. 2-D radiation patterns at the select frequencies.

spectra that generate from different types of defected models. Therefore, Fig. 8(a) shows the examples of detected UHF PD signals of the

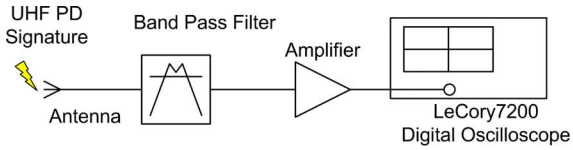

Fig. 5. Configuration of the UHF antenna system.

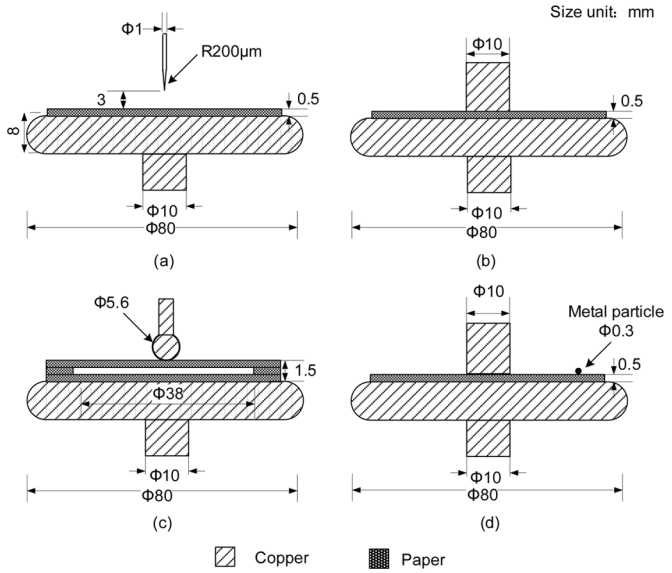

Fig. 6. Four types of artificial defect models: (a) Corona-in-oil discharge model; (b) Surface discharge-in-oil model; (c) Gas-cavity discharge model; (d) Floating-discharge-in-oil model.

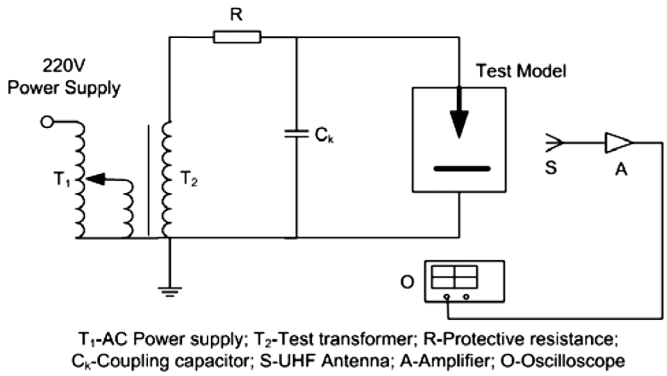

Fig. 7. The setup of PD experiment in laboratory.

four defect models. The waveforms of the UHF PD signals before 100 ns are the background noises. The four PD signals seem similar to each other but differ in details. Examples of normalized power frequency spectra of the UHF PD signals of the four defected models, as shown in Fig. 8(b), are obviously different. The results indicate that the proposed UHF antenna is effective in capturing PD waveforms. And the UHF PD signals can be used for recognition by analysis to the waveforms.

IV. Conclusion

This communication presents a compact fourth order UHF Hilbert fractal antenna for PD online monitoring of transformers. The actual antenna was developed based on the optimal design procedure. The actual PD experiments including four typical artificial insulation defect

TABLE II
PD Experimental Conditions

Defect model	Inception voltage (kV)	Breakdown voltage (kV)	Test voltage (kV)	Sample numbers
Corona discharge	5.7	12.5	7.0	50
			8.0	50
			9.0	50
Surface discharge	8.4	13.2	9.0	50
			10.0	50
			11.0	50
Gas-cavity discharge	3.5	7.8	5.0	50
			6.0	50
			7.0	50
Floating discharge	6.8	11.5	8.0	50
			9.0	50
			10.0	50

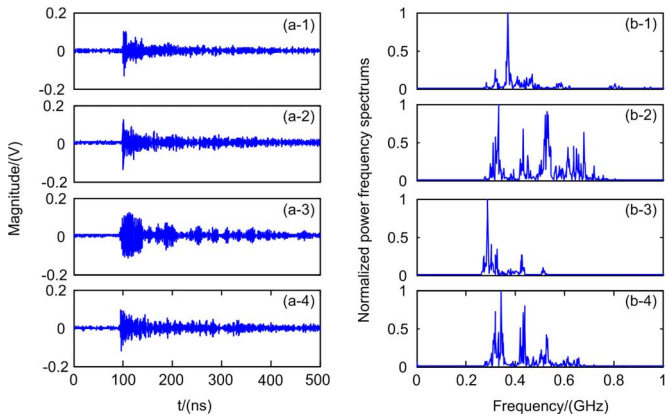

Fig. 8. Waveforms and normalized power frequency spectra of UHF PD signals: (1) Corona-in-oil discharge model; (2) Surface discharge-in-oil model; (3) Gas-cavity discharge model; (4) Floating-discharge-in-oil model.

models were carried out to verify the performance of the antenna. The results of the work can be summarized as follows:

a) The frequency pass band of the developed Hilbert fractal antenna is a few hundred MHz. And the radiation patterns show that the antenna can receive electromagnetic waves from the front of the antenna.
b) The gain variations of the optimal antenna at the three frequencies are relatively stable. The antenna can match with a 50 ohms coaxial cable well in the pass bands.
c) The experimental results show that the proposed antenna is effectively applied for UHF PD online monitoring of transformers. And the UHF PD signals measured by the proposed antenna can be used for recognition of PDs.

For future work, the detailed reason of low gain will be investigated and there is still scope for improvement in manufacturing an antenna with higher gain. Recognition of UHF PD signals are also needed for further studying.

References

[1] S. Tenbohlen, D. Denissov, S. M. Hoek, and S. M. Markalous, "Partial discharge measurement in the ultra high frequency (UHF) range," *IEEE Trans. Dielectr. Electr. Insul.*, vol. 15, pp. 1544–1552, Dec. 2008.
[2] F. H. Kreuger, *Partial Discharge Detection in High-Voltage Equipment*. London: Butterworths, 1989.
[3] G. Wang, Y. Zheng, Y. Hao, and Y. Li, "Study on the ultra-high-frequency sensor for PD detection in power transformer," in *Proc. Chinese Soc. Electr. Eng.* (in Chinese), 2004, vol. 22, pp. 154–160.

[4] G. P. Cleary and M. D. Judd, "UHF and current pulse measurements of partial discharge activity in mineral oil," in *Proc. Inst. Elect. Eng. Sci. Meas. Technol.*, 2006, vol. 53, pp. 47–54.
[5] C. Sun, G. Xu, J. Tang, H. Shi, and W. Zhu, "Model and performance of inner sensors used for partial discharge detection in GIS," in *Proc. Chinese Soc. Electr. Eng.* (in Chinese), 2004, vol. 24, pp. 89–94.
[6] Z. Jin, C. Sun, C. Cheng, and J. Li, "Two types of compact UHF antennas for partial discharge measurement," in *Proc. Int. Conf. High Voltage Eng. Appl.*, Chongqing, China, 2008, pp. 616–620.
[7] K. J. Vinoy, K. A. Jose, V. K. Varadan, and V. V. Varadan, "Resonant frequency of Hilbert curve fractal antennas," in *Proc. IEEE Antennas Propag. Soc. Int. Symp.*, Boston, 2001, pp. 648–651.
[8] J. Zhu, A. Hoorfar, and N. Enghata, "Bandwidth, cross-polarization and feed-point characteristics of matched Hilbert antennas," *IEEE Antennas Wireless Propag. Lett.*, vol. 2, pp. 2–5, 2003.
[9] X. Chen, S. N. Safieddin, and Y. Liu, "A down-sized printed Hilbert antenna for UHF band," in *Proc. IEEE Antennas Propag. Soc. Int. Symp.*, Columbus, 2003, pp. 581–584.
[10] T. Cui, W. Lin, H. Yin, and G. Wu, "Analysis on influencing factors to properties of UHF Hilbert fractal antenna," in *Proc. Int. Conf. High Voltage Eng. Appl.*, New Orleans, 2010, pp. 228–231.
[11] J. Li, J. Ning, Z. Jin, Y. Wang, and M. Li, "Research on UHF Hilbert fractal antenna for online transformer PD monitoring," (in Chinese) *Electr. Power Autom. Equip.*, vol. 27, pp. 31–35, Jun. 2007.

A Fixed-Frequency Beam-Steerable Half-Mode Substrate Integrated Waveguide Leaky-Wave Antenna

Asanee Suntives and Sean V. Hum

***Abstract*—A single-layer design of a half-mode substrate integrated waveguide (HMSIW) leaky-wave antenna (LWA) possessing fixed-frequency beam steering capability is presented in this communication. The antenna is loaded by series and shunt capacitive tuning elements, providing two degrees of freedom in which its dispersion characteristic can be manipulated. An antenna with a length of 3.25 λ_0 was implemented using fixed capacitors and experimentally validated. The measurements demonstrate a beam steering range between -31° and $+35^\circ$ at 6.5 GHz. The measured antenna gain is shown to be better than 9.5 dBi with circular polarization.**

***Index Terms*—Beam steering, leaky-wave antennas, metamaterials, reconfigurable antennas, substrate integrated waveguide.**

I. Introduction

A leaky-wave antenna (LWA) is a traveling-wave structure that radiates electromagnetic waves as they propagate along the antenna [1]. This type of antenna is much simpler to implement than conventional antenna arrays due to the series feeding of the elements. More recently, in the microwave and millimeter-wave frequency regimes, substrate integrated waveguide (SIW) and half-mode SIW (HMSIW) structures have become popular candidates for implementing antennas to take advantage of their low-loss characteristics and compatibility with other SIW-based circuits [2]–[6].

Recent advances in LWAs enable a frequency-scanning capability that can steer the antenna beam from backward to forward directions by employing metamaterial structures. However, most wireless applications nowadays are designed to operate in certain allocated frequency bands. Therefore, there are increasing needs for fixed-frequency beam steerable LWAs. For instance, this type of LWA can be implemented by loading the structure with electrically tunable elements, usually varactor diodes [7]–[9]. A LWA that produces beam steering between near-broadside and forward angles has been developed previously [8]. The edge of a microstrip line is grounded on one side, and the other edge is loaded with capacitors. The resulting LWA produces beam steering between near-broadside and forward angles. While the grounded microstrip LWA resembles a HMSIW, the base structure is not a metamaterial and, hence, not capable of scanning backward. Hence, we have recently proposed a HMSIW LWA that provides this capability [9]. A metamaterial can be readily realized using HMSIW, since its base structure can accommodate both series and shunt tuning elements. These elements can be tuned to manipulate its dispersion characteristic allowing backward, broadside or forward beam angles. The proposed concept was demonstrated experimentally with a unit cell prototype proving the electrical tunability of the device [9]. However, the antenna was implemented using two substrate layers that required more fabrication steps.

In this communication, a new design of fixed-frequency electronically beam-steerable HMSIW LWA is presented. By incorporating interdigital capacitors in place of embedded patches in the series branch, the antenna can be easily implemented on a single substrate layer. The proposed antenna structure and its dispersion characteristics are discussed in Section II. Full-wave analysis of the antenna performance is presented in Section III. Finally, in the same section, an experimental characterization of full-length antenna prototypes implemented using fixed capacitors is presented.

II. Proposed Unit Cell Design

In order for a LWA operating in its principal mode to scan in the backward and forward directions, the guided-wave structure must exhibit the same dispersion characteristic to that of a metamaterial transmission line [10]. This implies that over a range of frequencies the phase constant is negative, i.e. backward scanning, and it becomes positive, i.e. forward scanning, as the frequency passes the transition point. The angle of the maximum of the beam measured from broadside (θ) can be estimated from [1]

$$\theta = \sin^{-1}(\beta/k_o) \tag{1}$$

where k_o is the free space wavenumber, β is the phase constant, and the guided wave becomes leaky when $\beta/k_o < 1$.

Fig. 1 shows two cells of the proposed antenna structure. Typically, a metamaterial transmission line is achieved by adding series capacitive and shunt inductive elements [10]. In this case, the series interdigital capacitors and shunt capacitors connected to ground vias provide those necessary conditions. Previously, the fixed series capacitive elements were formed by inter-layer coupling patches, which complicated the fabrication process [9]. To manipulate the dispersion characteristic of a waveguide structure, the most obvious way is to change its cutoff frequency. Therefore, each antenna unit cell is loaded by a capacitive tuning element in a shunt manner, i.e., C_{sh} [11]. Since an SIW is essentially a closed structure whose shunt branches are not easily accessible,

Manuscript received May 21, 2011; revised October 03, 2011; accepted November 15, 2011. Date of publication March 01, 2012; date of current version May 01, 2012. This work was supported by the Natural Sciences and Engineering Research Council (NSERC) of Canada.

The authors are with the Edward S. Rogers Sr. Department of Electrical and Computer Engineering, University of Toronto, Toronto, ON M5S 3S4, Canada (e-mail: asanee.suntives@mail.mcgill.ca; svhum@waves.utoronto.ca).

Color versions of one or more of the figures in this communication are available online at http://ieeexplore.ieee.org.

Digital Object Identifier 10.1109/TAP.2012.2189726